Self-Assembly of a Porphyrin Array via the Molecular Recognition Approach: Synthesis and Properties of a Cyclic Zinc(II) Porphyrin Trimer Based on Coordination and Hydrogen Bonding

Chusaku Ikeda,*,† Yuichi Tanaka,† Takeshi Fujihara,† Yoko Ishii,† Takeshi Ushiyama,† Kimihisa Yamamoto,‡ Naoki Yoshioka,† and Hidenari Inoue†

Department of Applied Chemistry, and Department of Chemistry, Keio University, 3-14-1 Hiyoshi Kohoku-ku, Yokohama 223-8522, Japan

Received December 18, 2000

Self-assembly of [5-(pyrazol-4-yl)-10,20-bis(*p*-tolyl)-15- (2-ethoxycarbonylphenyl)porphyrinato]-zinc(II) (**1**), designed to have both a coordination site and a hydrogen bonding site, leads to a stable cyclic trimer array where coordination of the pyrazole nitrogen to the zinc(II) ion as well as hydrogen bonding between carbonyl oxygen and pyrazole NH holds each zinc(II) porphyrin. The recognition event for pyrazole has been confirmed preliminarily in the model studies using [5-(2-ethoxycarbonylphenyl)tris(*p*-tolyl)porphyrinato]-zinc(II) (**3**). The zinc(II) porphyrin **3** has large affinity for pyrazole due to the hydrogen bond between pyrazole and the 2-ethoxycarbonyl group in addition to the coordination bonding accompanied by the conformational change of the ethoxycarbonyl group in the coordination process. The ^{1}H NMR, IR, and UV−vis spectra of **1** and its ESI-MS and VPO measurements have revealed the cyclic trimer structure with an overall association constant of 6.0×10^{13} M^{-2} at 22 °C. The contribution of the hydrogen bond to the total free energy change in trimer formation is estimated to be 7.5 kcal/mol based on a reference trimer system without a hydrogen bonding site. The trimer geometry causes characteristic exitonic interaction between porphyrin units to yield a broad Soret band which is deconvoluted into four components by UV−vis and MCD spectral analyses. Electrochemical measurements have shown that only the first ring-oxidation process proceeds stepwise in the trimer.

Introduction

In recent years, there has been increasing interest in constructing well-organized porphyrin assemblies because several types of multi porphyrin systems with a well-controlled geometry play a crucial role in the energy and/or electron-transfer properties in the photosynthetic process.[1] Inspired by the beautiful X-ray crystallographic structures of the natural photosynthetic systems,[1f,g] numerous porphyrin assemblies have been synthesized to mimic some parts of their functions in which the distance and orientation between the chromophores are important.[1a−e]

Self-assembling strategies based on reversible, noncovalent interactions have been widely used as an alternative to covalent approaches for constructing the porphyrin assemblies since spontaneous association from relatively small and simple units easily leads to the construction of large-scale ordered arrays which will be hard to achieve only by covalent bond.[2,3,4] As far as the shapes of the self-assembled products are concerned, one-dimensional long linear chains,[5] two-dimensional sheet like structures[6] and three-dimensional cyclic or round shaped assemblies[7,8,9] are well-known as examples of the self-assembled porphyrin systems as well as other unique systems.[1c,10]

Particularly, cyclic porphyrin arrays are of great interest because their cyclic geometry may realize the large ring shaped

* Corresponding author. Present address: Graduate School of Materials Science, Nara Institute of Science and Technology (member of professor Yoshiaki Kobuke's group), 8916−5 Takayama, Ikoma, 630-0101, Japan. E-mail: chusaku@hotmail.com. Fax: (+81)-743-72-6119.

† Department of Applied Chemistry.

‡ Department of Chemistry.

(1) (a) Wasielewski, M. R. *Chem. Rev.* **1992**, *92*, 435. (b) Ward, M. D. *Chem. Soc. Rev.* **1997**, *26*, 365. (c) Blanco, M.-J.; Jiménez, M. C.; Chambron, J.-C.; Heitz, V.; Linke, M.; Sauvage, J.-P. *Chem. Soc. Rev.* **1999**, *28*, 293. (d) Hayashi, T.; Ogoshi, H. *Chem. Soc. Rev.* **1997**, *26*, 355. (e) Piotrowiak, P. *Chem. Soc. Rev.* **1999**, *28*, 143. (f) Deisenhofer, J.; Epp, O.; Miki, K.; Huber, R.; Michel, H. *J. Biol. Chem.* **1984**, *180*, 385. (g) Mcdermott, G.; Prince, S. M.; Freer, A. A.; Hawthornthwaite-Lawless, A. M.; Papiz, M. Z.; Cogdell, R. J.; Isaacs, N. W. *Nature* **1995**, *374*, 517.

(2) (a) Philp, D.; Stoddart, J. F. *Angew. Chem., Int. Ed. Engl.* **1996**, *35*, 1154. (b) Whitesides, G. M.; Mathias, J. P.; Seto, C. T. *Science* **1991**, *254*, 1312. (c) Lindsey, J. S. *New. J. Chem.* **1991**, *15*, 153.

(3) For recent reviews for porphyrin oligomers by noncovalent bond, see: (a) Ogoshi, H.; Mizutani, T.; Hayashi, T.; Kuroda, Y. In *The Porphyrin handbook*; Kadish, K. M., Smith, K. M., Guilard, R., Eds.; Academic Press: San Diego, 2000; Chapter 46. (b) Chambron, J.-C.; Heitz, V.; Sauvage, J.-P. In *The Porphyrin handbook*; Kadish, K. M., Smith, K. M., Guilard, R., Eds.; Academic Press: San Diego, 2000; Chapter 40.

(4) (a) Bhyrappa, P.; Wilson, S. R.; Suslick, K. S. *J. Am. Chem. Soc.* **1997**, *119*, 8492. (b) Kobayashi, K.; Koyanagi, M.; Endo, K.; Masuda, H.; Aoyama, Y. *Chem. Eur. J.* **1998**, *4*, 417. (c) Goldberg, I. *Chem. Eur. J.* **2000**, *6*, 3863.

(5) (a) Fleisher, E. B.; Shachter, A. M. *Inorg. Chem.* **1991**, *30*, 3763. (b) Burrell, A. K.; Officer, D. L.; Reid, D. C. W.; Wild, K. Y. *Angew. Chem., Int. Ed. Engl.* **1998**, *37*, 114. (c) Michelsen, U.; Hunter, C. A. *Angew. Chem., Int. Ed.* **2000**, *39*, 764. (d) Nagata, N.; Kugimiya, S.; Kobuke, Y. *Chem. Commun.* **2000**, 1389. (e) Ogawa, K.; Kobuke, Y. *Angew. Chem., Int. Ed.* **2000**, *39*, 4070.

(6) (a)Drain, C. M.; Lehn, J.-M. *J. Chem. Soc., Chem. Commun.* **1994**, 2313. (b) Stang, P. J.; Fan, J.; Olenyuk, B. *Chem. Commun.* **1997**, 1453. (c) Drain, C. M.; Nifiatis, F.; Vasenko, A.; Batteas, J. D. *Angew. Chem., Int. Ed.* **1998**, *37*, 2344. (d) Fan, J.; Whiteford, J. A.; Olenyuk, B.; Levin, M. D.; Stang, P. J.; Fleischer, E. B. *J. Am. Chem. Soc.* **1999**, *121*, 2741. (e) Drain, C. M.; Shi, X.; Milic, T.; Nifiatis, F. *Chem. Commun.* **2001**, 287.

10.1021/ic001421k CCC: $20.00
Published on Web 06/06/2001

porphyrin assembly that would have insight into the function of bacteriochlorophyll ring assembly in the natural LH2 complex.[1g] Coordination of the peripheral substituent ligand to the porphyrin central metal ion is an effective means to construct such a class of cyclic assemblies.[11] A variety of cofacial dimers,[12,13] cyclic trimers,[8] and tetramers[8e,f,9] have been constructed using this strategy and reported.[14] Many studies of cofacial dimers containing biomimetic zinc(II) or magnesium(II) ions have clarified their specific optical or electrochemical properties by means of their structural dimensions as a model system of the "special pair" in the photosynthetic reaction center.[12,15] However, construction of larger cyclic oligomers containing biomimetic metal ions is still an active research area because the detailed studies of structure-induced properties of such cyclic oligomers have been restricted to those utilizing coordination of inert ions and the reported cyclic oligomers based on mutual coordination using zinc(II) ions were not so stable in a relatively dilute concentration range.[8e,f] Recently, we have reported the self-assemblies of pyrazole-substituted porphyrins by intermolecular hydrogen bond or metal−ligand coordination.[8f,16] We have extended our approach and designed zinc(II) pyrazolylporphyrin that can utilize both of coordination and hydrogen bonding. The large stability of the assemblies could be obtained owing to the cooperative action of these bonds and allows a detailed study of the geometry-induced spectroscopic or electrochemical properties. The design, synthesis, and thermodynamics of the porphyrin self-assemblies to recognize pyrazole are described in comparison with the reference systems.

Experimental Section

Materials. Pyrrole and *p*-tolualdehyde were purchased from Aldrich and distilled under reduced pressure prior to use. Deuteriochloroform ($CDCl_3$) stabilized with silver foil (Merk) was used as received for vapor pressure osmometry (VPO) measurements. Deuteriochloroform used in the NMR titration was passed through a short column (ca. 1 cm × 5 cm) of potassium carbonate and alumina (basic, grade I) prior to use. Dichloromethane was distilled from CaH_2. Dichloromethane for the spectroscopic measurements was of spectroscopic grade (Kanto Chemical) and used as received. All other solvents and chemicals were commercial materials and used without purification. Column Chromatography was performed on 70−230 mesh silica gel (Katayama Chemical) or 70−230 mesh neutral alumina (Merk). Alumina was deactivated to grade III prior to use. 1-*p*-Methoxybenzylpyrazol-4-carboxaldehyde (**5**),[17] meso-unsubstituted dipyrromethane (**7**),[18] *p*-tolyldipyrromethane (**15**),[19] 5-(pyrazolyl)-10, 15, 20-tris(*p*-tolyl)-porphyrin (**12**),[16] and tetrakis(*p*-tolyl)porphyrin (**14**)[20] were synthesized according to the published procedures.

Measurements. ^{1}H NMR spectra were recorded on a JEOL 300 MHz LABDA-300 spectrometer and chemical shifts are reported relative to internal TMS δ 0.0 ppm or to the signal of a residual protonated solvent: $CDHCl_2$ δ 5.32 ppm, $CHCl_3$ δ 7.26 ppm. IR spectra were obtained with an FTS-165 (BIORAD) spectrophotometer. UV−vis spectra were obtained on a JASCO V570 spectrophotometer equipped with a JASCO ETC-505T temperature controller using 10, 1.0, 0.1, and 0.025 mm quartz cells. Steady-state fluorescence spectra were obtained on an JASCO FP-777W spectrofluorometer. Emission lifetimes were measured by time-correlated single-photon counting with a nanosecond pulsed lamp and a Horiba NAES-550 photomultiplier. The magnetic circular dichroism (MCD) spectra were recorded on a JASCO V720 spectropolarimeter equipped with a JASCO MCD-317 water-cooled electromagnet (1.1 T) and magnetic shielding of the detector. Electron spray ionization mass (ESI MS) spectra were recorded on a JEOL JMS-700 mass spectrometer. Vapor pressure osmometry (VPO) measurements were performed on a KNAUAR K-7000 osmometer with tetraphenylporphyrin and benzil as standards. VPO measurements were performed between 5 mM and 20 mM in $CDCl_3$ at 26 °C.[21] Elemental analyses were performed at the Central Laboratory of Faculty of Science and Technology, Keio University. Cyclic voltammetry (CV) and differential pulse voltammetry (DPV) were performed with a ALS 660-A voltammetry analyzer. The working and counter electrodes for the electrochemical measurements were a platinum disk

(7) (a) Kariya, N.; Imamura, T.; Sasaki, Y. *Inorg. Chem.* **1997**, *36*, 833. (b) Johnston, M. R.; Gunter, M. J.; Warrener, R. N. *Chem. Commun.* **1998**, 2739. (c) Reek, J. N. H.; Schenning, A. P. H. J.; Bosman, A. W.; Meijer, E. W.; Crossley, M. J. *Chem. Commun.* **1998**, 11. (d) Knapp, S.; Vasudevan, J.; Emge, T. J.; Arison, B. H.; Potenza, J. A.; Schugar, H. J. *Angew. Chem., Int. Ed.* **1998**, *37*, 2368. (e) Robtsov, I. V.; Kobuke, Y.; Miyaji, H.; Yoshihara, K. *Chem. Phys. Lett.* **1999**, *308*, 323. (f) Alessio, E.; Geremia, S.; Mestroni, S.; Srnova, I.; Slouf, M.; Gianferrara, T.; Prodi, A. *Inorg. Chem.* **1999**, *38*, 2527. (g) Mak, C. C.; Bampos, N.; Sanders, J. K. M. *Chem. Commun.* **1999**, 1085. (h) Darling, S. L.; Mak, C. C.; Bampos, N.; Feeder, N.; Teat, S. J.; Sanders, J. K. M. *New. J. Chem.* **1999**, *23*, 359. (i) Chichak, K.; Branda, N. R. *Chem. Commun.* **2000**, 1211. (j) Haycock, R. A.; Yartsev. A.; Michelsen, U.; Sundström, V.; Hunter, C. A. *Angew. Chem., Int. Ed.* **2000**, *39*, 3616.

(8) (a) Wojaczyński, J.; Latos-Grażyński, L. *Inorg. Chem.* **1995**, *34*, 1044. (b) Wojaczyński, J.; Latos-Grażyński, L. *Inorg. Chem.* **1995**, *34*, 1054. (c) Wojaczyński, J.; Latos-Grażyński, L. *Inorg. Chem.* **1996**, *35*, 4812. (d) Wojaczyński, J.; Latos-Grażyński, L.; Olmstead, M. M.; Balch, A. L. *Inorg. Chem.* **1997**, *36*, 4548. (e) Chi, X.; Guerin, A. J.; Haycock, R. A.; Hunter, C. A.; Sarson, L. D. *J. Chem. Soc., Chem. Commun.* **1995**, 2567. (f) Ikeda, C.; Nagahara, N.; Yoshioka, N.; Inoue, H. *New J. Chem.* **2000**, *24*, 897.

(9) Funatsu, K.; Imamura, T.; Ichimura, A.; Sasaki, Y. *Inorg. Chem.* **1998**, *37*, 1798.

(10) (a) Anderson, H. L. *Inorg. Chem.* **1994**, *33*, 972. (b) Taylor, P. N.; Anderson, H. L. *J. Am. Chem. Soc.* **1999**, *121*, 11538.

(11) For the porphyrin rings using other approaches, see: (a) Biemans, H. A. M.; Rowan, A. E.; Verhoeven, A.; Vanoppen, P.; Latterini, L.; Foekema, J.; Shenning, A. P. H. J.; Meijer, E. W.; De Schryver, F. C.; Nolte, R. J. M. *J. Am. Chem. Soc.* **1998**, *120*, 11054. (b) Anderson, H. L.; Sanders, J. K. M. *J. Chem. Soc., Chem. Commun.* **1989**, 1714. (c) Li, J.; Ambroise, A.; Yang, S. I.; Diers, J. R.; Seth, J.; Wack, C. R.; Bocian, D. F.; Holten, D.; Lindsey, J. S. *J. Am. Chem. Soc.* **1999**, *121*, 8927.

(12) (a) Kobuke, Y.; Miyaji, H. *J. Am. Chem. Soc.* **1994**, *116*, 4111. (b) Hunter, C. A.; Sarson, L. D. *Angew. Chem., Int. Ed. Engl.* **1994**, *33*, 2313. (c) Stibrany, R. T.; Vasudevan, J.; Knapp, S.; Potenza, J. A.; Emge, T.; Schugar, H. J. *J. Am. Chem. Soc.* **1996**, *118*, 3980. (d) Gerasimchuk, N. N.; Mokhir, A. A.; Rodgers, K. R. *Inorg. Chem.* **1998**, *37*, 5641. (e) Gardner, M.; Guerin, A. J.; Hunter, C. A.; Michelsen, U.; Rotger, C. *New. J. Chem.* **1999**, *23*, 309.

(13) (a) Goff, H. M.; Shimomura, E. T.; Lee, Y. J.; Scheidt, W. R. *Inorg. Chem.* **1984**, *23*, 315. (b) Godziela, G. M.; Tilotta, D.; Goff, H. M.; *Inorg. Chem.* **1986**, *25*, 2142. (c) Aoyama, Y.; Kamohara, T.; Yamagishi, A.; Toi, H.; Ogoshi, H. *Tetrahedron Lett.* **1987**, *28*, 2143. (d) Balch, A. L.; Noll, B. C.; Olmstead, M. M.; Reid, S. M. *J. Chem. Soc., Chem. Commun.* **1993**, 1088. (e) Balch, A. L.; Latos- Grażyński, L.; St. Claire, T, N. *Inorg. Chem.* **1995**, *34*, 1395. (f) Funatsu, K.; Imamura, T.; Ichimura, A.; Sasaki, Y. *Inorg. Chem.* **1998**, *37*, 4986.

(14) For the other porphyrin oligomers using the axial coordination, see ref 7 and: (a) Chernook, A. V.; Shulga, A. M.; Zenkevich, E. I.; Rempel, U.; von Borczyskowski, C. *J. Phys. Chem.* **1996**, *100*, 1918. (b) Kobuke, Y.; Miyaji, H. *Bull. Chem. Soc. Jpn.* **1996**, *69*, 3563. (c) Funatsu, K.; Kimura, A.; Imamura, T.; Ichimura, A.; Sasaki, Y. *Inorg. Chem.* **1997**, *36*, 1625. (d) Kariya, N.; Imamura, T.; Sasaki, Y. *Inorg. Chem.* **1998**, *37*, 1658. (e) Alessio, E.; Geremia, S.; Mestroni, S.; Iengo, E.; Sronova, I.; Slouf, M. *Inorg. Chem.* **1999,** *38*, 869. (f) Giribabu, L.; Rao, T. A.; Maiya, B. G. *Inorg. Chem.* **1999**, *38*, 4971. (g) Kim, H.-J.; Bampos, N.; Sanders, J. K. M. *J. Am. Chem. Soc.* **1999**, *121*, 8120.

(15) Recently, bacteriochlorophyll containing zinc(II) ion was discovered: Wakao, N.; Yokoi, N.; Isoyama, N.; Hiraishi, A.; Shimada, K.; Kobayashi, M.; Kise, H.; Iwaki, M.; Itoh, S.; Takaichi, S.; Sakurai, Y. *Plant. Cell Phys.* **1996**, *37*, 889.

(16) Ikeda, C.; Nagahara, N.; Motegi, E.; Yoshioka, N.; Inoue, H. *Chem. Commun.* **1999**, 1759.

(17) Werner, A.; Sánchez-Migallón, A.; Fruchier, A.; Elguero, J.; Fernández- Castaño, C.; Foces-Foces, C. *Tetrahedron*, **1995**, *51*, 4779.

(18) Wang, Q. M.; Bruce, D. W. *Synlett* **1995**, 1267.

(19) (a) Lee, C.-H.; Lindsey, J. S. *Tetrahedron* **1994**, *50*, 11427. (b) Littler, B. J.; Miller, M. A.; Hung, C.-H.; Wagner, R. W.; O'Shea, D. F.; Boyle, P. D.; Lindsey, J. S. *J. Org. Chem.* **1999**, *64*, 1391.

(20) Adler, A.; Longo, F. R.; Shergalis, W. *J. Am. Chem. Soc.* **1964**, *86*, 3145.

(i.d. = 1.5 mm) and a platinum wire, respectively. Cyclic voltammograms were recorded at a scan rate of 100 mV/s at ambient temperature, and differential pulse voltammograms were recorded with a pulse width of 5 mV. The sample solutions (1 mM) in CH_2Cl_2 containing 0.1 M TBA·BF_4 (tetrabulylammonium tetrafluoroborate) were deoxygenated by an argon stream. The reference electrode was Ag/Ag^+ and the potentials reported here are with respect to this reference electrode, against which the redox potential of ferrocenium−ferrocene was 0.204 V. The peak deconvolution analysis of absorption and MCD spectra and of DPV data was carried out using the program PEAKFIT version 4 (SPSS. Inc.). Geometry optimization for CPK modeling was performed using the MOPAC III program (Fujitsu Ltd.). The characteristic features of the zinc(II) ion in the axially coordinated system studied included the displacement of the zinc(II) ion from the four nitrogen plane (0.35−0.38 Å). The structural parameters are in a range found for zinc(II) porphyrin by X-ray crystallography.[22]

5-(*p*-Methoxybenzylpyrazol-4-yl)-15-(2-ethoxycarbonylphenyl) Porphyrin (8). A 500 mL round-bottomed flask was charged with **5** (0.17 g, 0.88 mmol), ethyl 2-formylbenzoate **6** (0.15 g, 0.88 mmol), and **7** (0.25 g, 1.72 mmol) and dichloromethane (330 mL). After bubbling with an Ar stream, a catalytic amount of TFA (83.2 μL, 1.1 mmol) was added. After stirring for 3 h under dark conditions, 499 mg (2.2 mmol) of DDQ was added and the reaction mixture was further stirred for 1h. The reaction mixture was evaporated to dryness and the obtained residue was purified by column chromatography on silica gel with dichloromethane as eluent. Additional purification using alumina eluted with dichloromethane/*n*-hexane (1:2) followed by recrystallization from dichloromethane/*n*-hexane gave the title compound. Yield: 108 mg (19%). Mp: 198 °C. ^{1}H NMR (300 MHz, $CDCl_3$) δ 10.22 (s, 2H, 10- and 20-*meso*), 9.38−9.24 (each d, J = 4.6 Hz, 2H × 3, pyrrole-H_β), 8.87 (d, J = 4.6 Hz, 2H, pyrrole-H_β), 8.44, 8.16 (each s, 1H × 2, H_3 and H_5 in pyrazolyl), 8.40 and 8.19 (each m, 1H × 2, H_3 and H_6 in 2-ethoxycarbonylphenyl), 7.86 (m, 2H, H_4 and H_5 in 2-ethoxycarbonylphenyl), 7.50 and 7.03 (each d, J = 8.5 Hz, 2H × 2, H_o and H_m in *p*-methoxybenzyl), 5.64 (s, 2H, N−CH_2 in *p*-methoxybenzyl), 3.84 (s, 3H, OMe), 3.06 (q, J = 7.0 Hz, 2H, CH_2 in ethyl), −0.74 (t, J = 7.0 Hz, 3H, CH_3 in ethyl), −3.02 (br. s, 2H, inner NH). Anal. Calcd for $C_{40}H_{32}N_6O_3$·H_2O: C, 72.49; H, 5.17; N, 13.04. Found: C, 72.68; H, 5.00; N, 12.59.

5-(*p*-Methoxybenzylpyrazol-4-yl)-10,20-dibromo-15- (2-ethoxycarbonylphenyl) Porphyrin (9). A 100 mL round-bottom flask was charged with 0.11 g (0.17 mmol) of **8**, 50 mL of chloroform, and 0.2 mL of pyridine. After the mixture was cooled to 0 °C, *N*-bromosuccinimide (80 mg, 0.44 mmol) was added and the reaction mixture was stirred for 10 min followed by adding 4 mL of acetone. After evaporation to dryness, the obtained residue was washed with methanol. The crude mixture was purified by column chromatography on silica gel with dichloromethane as eluent. Recrystallization from dichloromethane/*n*-hexane gave the title compound. Yield: 104 mg (77%). Mp: 126−128 °C. ^{1}H NMR (300 MHz, $CDCl_3$) δ 9.62, 9.55, 9.05, and 8.64 (each d, J = 4.9 Hz, 2H × 4, pyrrole-H_β), 8.35 and 8.14 (each s, 1H × 2, H_3 and H_5 in pyrazolyl), 8.42 and 8.10 (m, 1H × 2, H_3 and H_6 in 2-ethoxycarbonylphenyl), 7.88 (m, 2H, H_4 and H_5 in 2-ethoxycarbonylphenyl), 7.53 and 7.05 (each d, J = 8.5 Hz, 2H × 2, H_o and H_m in *p*-methoxybenzyl), 5.66 (s, 2H, N−CH_2 in *p*-methoxybenzyl), 3.87 (s, 3H, OMe), 3.22 (q, J = 7.0 Hz, 2H, CH_2 in ethyl), −0.43 (t, J = 7.0 Hz, 3H, CH_3 in ethyl), −2.64 (br. s, 2H, inner NH). Anal. Calcd for $C_{40}H_{30}N_6O_3Br_2$·$0.5H_2O$: C, 59.20; H, 3.85; N, 10.36. Found: C, 59.07; H, 4.03; N, 9.98.

5-(*p*-Methoxybenzylpyrazol-4-yl)-10,20-di(*p*-tolyl)-15-(2-ethoxy- carbonylphenyl) Porphyrin (10). A 200 mL round-bottom flask with a reflux condenser was charged with **9** (117 mg, 0.15 mmol), tetrakis(triphenylphosphine)palladium (113 mg, 0.1 mmol), and benzene (60 mL). After adding of Na_2CO_3 (aq) (2 M, 18.5 mL) and a solution of 4-methylphenylboronic acid (2.52 g, 18.53 mmol) dissolved in 11.3 mL of ethanol by ultrasound sonication, the reacition mixture was refluxed for 20 h at 80 °C under N_2. Then the reaction mixture was diluted with water and benzene. The organic layer was separated, washed with water, and dried over Na_2SO_4. After the layer was evaporated to dryness, the obtained residue was purified by column chromatography on silica gel with dichloromethane as eluent. Recrystallization from dichloromethane/*n*-hexane gave the title compound. Yield: 56 mg (46%). Mp: 165−170 °C. ^{1}H NMR (300 MHz, $CDCl_3$) δ 9.04, 8.87, 8.82, and 8.63 (each d, J = 4.6 Hz, 2H × 4, pyrrole-H_β), 8.36 and 7.95 (each s, 1H × 2, H_3 and H_5 in pyrazolyl), 8.32 and 8.10 (m, 1H × 2, H_3 and H_5 in 2-ethoxycarbonylphenyl), 8.04(m, 4H, H_o in *p*-tolyl), 7.68 (m, 2H, H_4 and H_5 in 2-ethoxycarbonylphenyl), 7.45 (m, 4H, H_m in *p*-tolyl), 7.24 and 6.83 (each d, 2H × 2, H_o and H_m in *p*-methoxybenzyl), 5.58 (s, 2H, N−CH_2 in *p*-methoxybenzyl), 3.82 (s, 3H, OMe), 3.16 (q, J = 7.0 Hz, CH_2 in ethyl), 2.69 (s, 6H, CH_3 in *p*-tolyl), −0.52 (t, J = 7.0 Hz, CH_3 in ethyl), −2.70 (br. s, 2H, inner NH).

5-(Pyrazol-4-yl)-10,20-di(*p*-tolyl)-15-(2-ethoxycarbonylphenyl) Porphyrin (11). A solution of **10** (75 mg, 0.09 mmol) in 70 mL of TFA was refluxed for 48 h under N_2 in a three-necked round-bottom flask equipped with a condenser. After the mixture was neutralized with saturated $NaHCO_3$ (aq), the reaction mixture was diluted with chloroform and the organic layer was washed with water and dried over Na_2SO_4. After the layer was evaporated to dryness, the obtained residue was purified by column chromatography on silica gel with toluene/ethyl acetate (3:1). Recrystallization from dichloromethane/*n*-hexane gave the title compound. Yield: 27 mg (42%). Mp: 259−263 °C. ^{1}H NMR (300 MHz, $CDCl_3$) δ 8.96, 8.86, 8.82, and 8.64 (each d, J = 4.6 Hz, 2H × 4, pyrrole-H_β), 8.27(s, 2H, H_3 and H_5 in pyrazolyl), 8.40 and 8.15 (m, 1H × 2, H_3 and H_6 in 2-ethoxycarbonylphenyl), 8.08 (m, 4H, H_o in *p*-tolyl), 7.85(m, 2H, H_4 and H_5 in 2-ethoxycarbonylphenyl), 7.55(d, 4H, H_m in *p*-tolyl), 3.20(q, J = 7.0 Hz, CH_2 in ethyl), 2.71(s, 6H, CH_3 in *p*-tolyl), −0.46(t, J = 7.0 Hz, 3H, CH_3 in ethyl), −2.69(br. s, 2H, inner-NH). Anal. Calcd. for $C_{46}H_{36}N_6O_2$ $0.5H_2O$: C, 77.40; H, 5.22; N, 11.77. Found: C, 76.96; H, 5.35; N, 11.41.

Zinc(II) 5-(Pyrazol-4-yl)-10,20-di(*p*-tolyl)-15-(ethoxybenzyl) Porphyrin (1). Zinc(II) acetate (4.89 g, 22.3 mmol) dissolved in methanol (100 mL) was added to a solution of **11** (314.6 mg, 0.45 mmol) in 200 mL of chloroforom. After the mixture was stirred and refluxed for 10 h, the reaction mixture was diluted with chloroform and water. The organic layer was separated and dried over Na_2SO_4. After the layer was evaporated to dryness, the obtained residue was purified by column chromatography on alumina with dichloromethane/*n*-hexane (1:2). Recrystallization from dichlromethane/*n*-hexane gave the title compouned. Yield: 153 mg (48%). Mp > 300 °C. ^{1}H NMR (300 MHz, CD_2Cl_2) δ 8.89, 8.72, 8.60 (each d, J = 4.6 Hz, 2H × 3, pyrrole-H_β), 8.47 and 8.43 (each dd, 1H × 2, H_3 and H_6 in 2-ethoxycarbonylphenyl), 8.33 (d, J = 7.5 Hz, 2H, H_o in *p*-tolyl), 7.96 (d, 2H, H_o in *p*-tolyl, partially overlapped with H_4 and H_5 in 2-ethoxycarbonylphenyl), 7.87−7.94 (m, 2H, H_4 and H_5 in 2-ethoxycarbonylphenyl), 7.61 and 7.57 (each d, 2H × 2, partially overlapped with each other, H_m in *p*-tolyl), 7.21 (d, J = 4.6 Hz, 2H, pyrrole-H_β), 6.85 (br.s, 1H, pyrazole NH), 6.39 (s, 1H, H_5 in pyrazolyl), 3.77 (q, J = 7.0 Hz, 2H, CH_2 in ethyl), 2.80 (s, 6H, CH_3 in *p*-tolyl), 2.47 (s, 1H, H_3 in pyrazolyl), 1.00 (t, J = 7.0 Hz, 3H, CH_3 in ethyl). Anal. Calcd for $C_{46}H_{34}N_6O_2Zn$·$1.5H_2O$: C, 69.48; H, 4.69; N, 10.57. Found: C, 69.89; H, 4.69; N, 10.08.

Results and Discussion

Preparation of Porphyrins. At first, we attempted to synthesize **1** by condensation of tolyldipyrromethane (**15**), pyrazolaldehyde (**5**), and formylbenzoate (**6**). However, the purification of the desired compound from the reaction mixture was unsuccessful due to the formation of "scrambled" products.[23] Therefore, **1** was obtained by stepwise synthesis via a *meso* unsubstituted porphyrin precursor to avoid the scrambling

(21) $CDCl_3$ stabilized with silver foil was used for the solvent because the measurement could not be performed in dichloromethane (too low boiling point), and nonstabilized chloroform sometimes decomposes the sample. Chloroform stabilized with ethanol was also avoided since ethanol weakens the hydrogen bond in the assembly. UV−vis and ^{1}H NMR studies indicate that the same assemblies are formed in chloroform and dichloromethane.

(22) Collins, D. M.; Hoard, J. L. *J. Am. Chem. Soc.* **1970**, *92*, 3761.

(23) Littler, B. J.; Ciringh, Y.; Lindsey, J. S. *J. Org. Chem.* **1999**, *64*, 2864.

Table 1. Thermodynamic Parameters of Host−Guest Complexation in Dichloromethane[a]

ligand	porphyrin	T (°C)	K (M^{-1})	ΔG (kcal mol^{-1})	ΔH (kcal mol^{-1})	$T\Delta S$ (kcal mol^{-1})
pyrazole	**3**	2	$(5.07 \pm 0.10) \times 10^4$			
		12	$(2.40 \pm 0.04) \times 10^4$			
		22	$(1.18 \pm 0.01) \times 10^4$	−5.52	−11.57	−6.05
		33	$(5.98 \pm 0.07) \times 10^3$			
	4	2	$(3.52 \pm 0.18) \times 10^3$			
		12	$(2.17 \pm 0.22) \times 10^3$			
		22	$(1.16 \pm 0.16) \times 10^3$	−4.15	−9.15	−5.00
		33	$(6.60 \pm 0.20) \times 10^2$			
pyridine	**3**	2	$(2.75 \pm 0.27) \times 10^4$			
		12	$(1.38 \pm 0.31) \times 10^4$			
		22	$(6.94 \pm 0.72) \times 10^3$	−5.18	−11.04	−5.86
		33	$(3.57 \pm 0.42) \times 10^3$			
	4	2	$(2.71 \pm 0.21) \times 10^4$			
		12	$(1.30 \pm 0.12) \times 10^4$			
		22	$(6.38 \pm 0.53) \times 10^3$	−5.15	−11.46	−6.31
		33	$(3.26 \pm 0.54) \times 10^3$			

[a] Free energy (ΔG) and entropy changes ($T\Delta S$) are calculated at 22 °C.

Scheme 1[a]

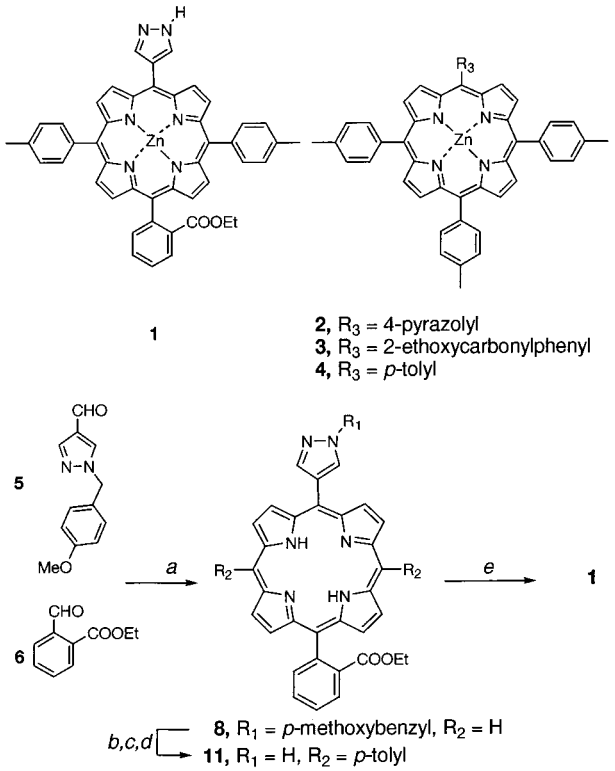

[a] Reagents and Conditions: (a) **7** TFA/CH_2Cl_2, then DDQ; (b) *N*-bromosuccinimide, pyridine/CH_2Cl_2; (c) 4-methylphenylboronic acid $Pd(PPh_3)_4/Na_2CO_3$/benzene; (d) TFA; (e) $Zn(CH_3COO)_2$/MeOH, CH_2Cl_2.

as shown in Scheme 1. The bromination of *meso* positions[24] and introduction of *p*-tolyl groups[25] were carried out by the reported procedure. Pyrazolylporphyrin **2** without any ethoxycarbonyl group and **3** with an ethoxycarbonylphenyl group instead of a pyrazole group were designed as reference compounds. **3** was synthesized using tolyldipyrromethane (**15**) and the appropriate aldehydes according to the reported procedure but with increased concentrations.[19a,26] **2** and **4** were synthesized via condensation of pyrrole and the appropriate aldehyde in refluxing propionic acid.[20] All the compounds showed sufficient solubility in chloroform and dichloromethane but poor solubility in toluene and benzene.

Binding Affinity of 3 for Pyrazole Ligand. From our previous work, it is apparent that the strength of axial coordination of pyrazole to the zinc(II) ion is greater than that of the hydrogen bond of pyrazole. Therefore we designed the molecular unit in which hydrogen bond to the pyrazole NH group supports the axially bonded pyrazole ligand. For this purpose, an ethoxycarbonyl group was introduced to the *ortho* position of the meso-aryl group as a proton acceptor substituent to recognize the pyrazole NH group.[27] Before taking into consideration the self-assembling properties of **1**, we studied the binding properties of the molecular unit with a pyrazole ligand using reference porphyrin **3**. The binding constants of **3** to pyrazole ligand were determined by the UV−vis spectroscopic titration method in dichloromethane.[28] The titration of **4** by pyridine ligand was also carried out as a reference. As when adding pyrazole to **3**, Soret and Q-bands were red shifted from 420 to 429 nm, 550 to 564 nm, and 589 to 605 nm in the B(0,0), Q(1,0), and Q(0,0) band, respectively, with isosbestic points. The shifts are characteristic of axial coordination of zinc(II) porphyrin, indicating the formation of a 1:1 complex with pyrazole. Similar spectral changes were observed for other titrations. The binding constants, K, and thermodynamic parameters, ΔG, ΔH, and $T\Delta S$ in dichloromethane at 295 K are summarized in Table 1. The enthalpy and entropy changes were calculated from the slope and intercept of the van't Hoff plots, which showed a linear relationship between $1/T$ and $\ln K$ in the range of 275−306 K. The binding constants of **3** with pyridine were much the same as those observed in **4** with pyridine, suggesting that the electron accepting property of the zinc(II) ion is not so altered by adding an ethoxycarbonyl substituent.[29] In contrast, **3** showed ca.10-fold larger binding constants for

(24) DiMagno, S. G.; Lin, V. S.-Y.; Therien, M. J. *J. Am. Chem. Soc.* **1993**, *115*, 2513.
(25) (a)Miyaura, N.; Yanagi, T.; Suzuki, A. *Synth. Commun.* **1981**, *11*, 513. (b) Zhou, X.; Chan, K. S. *J. Chem. Soc., Chem. Commun.* **1994**, 2493. (c) Hayashi, T.; Miyahara, T.; Koide, N.; Kato, Y.; Masuda, H.; Ogoshi, H. *J. Am. Chem. Soc*. **1997**, *119*, 7281.
(26) (a) Li, F.; Yang, K.; Tyhonas, J. S.; MacCrum, K. A.; Lindsey, J. S. *Tetrahedron* **1997**, *53*, 12339. (b) Lindsey, J. S.; MacCrum, K. A.; Tyhonas, J. S.; Chuang, Y.-Y. *J. Org. Chem.* **1994**, *59*, 579.
(27) For the pioneering molecular recognition using axial coordination and hydrogen bonding, see: (a) Boner-Law, R. P.; Sanders, J. K. M. *J. Chem. Soc., Chem. Commun.* **1991**, 574. (b) Mizutani, T.; Ema, T.; Tomita, T.; Kuroda, Y.; Ogoshi, H. *J. Chem. Soc., Chem. Commun.* **1993**, 520. (c) Mizutani, T.; Ema, T.; Yoshida, T.; Kuroda, Y.; Ogoshi, H. *Inorg. Chem.* **1993**, *32*, 2072. (d) Mizutani, T. Ema, T.; Tomita, T.; Kuroda, Y.; Ogoshi, H. *J. Am. Chem. Soc.* **1994**, *116*, 4240. (e) Bonar-Law, R. P.; Sanders, J. K. M. *J. Am. Chem. Soc.* **1995**, *117*, 259.
(28) Conner, K. A. *Binding Constants*, Wiley: New York, 1987.
(29) For the influences of the substituent effect in aryl groups on the axial coordination strength, see: Vogel, G. C.; Beckmann B. A. *Inorg. Chem.* **1976**, *15*, 483.

Scheme 2

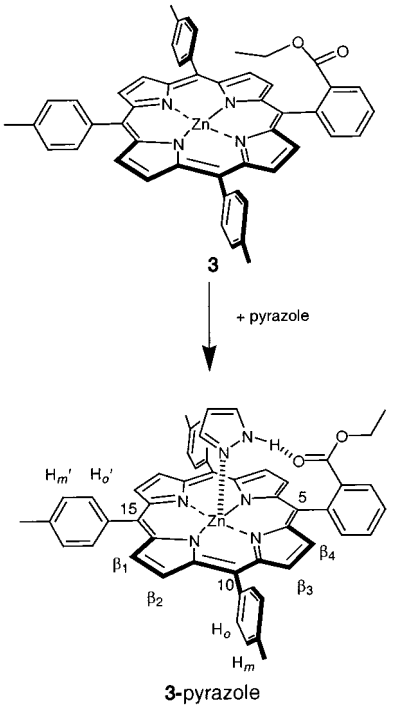

pyrazole than **4**. The ΔG and ΔH values for complexation between **3** and pyrazole are negatively larger than that between **4** and pyrazole, showing that the introduction of an ethoxycarbonyl group leads to the favorable increase in the affinity probably due to the hydrogen bonding. In addition, formation of hydrogen bond between pyrazole NH group and carbonyl oxygen in the ethoxycarbonyl group of **3** was confirmed. The carbonyl stretching band of **3,** observed at 1730 cm^{-1} in the absence of pyrazole, appeared at the lower frequency side (1715 cm^{-1}) when recorded with excess pyrazole.[30] These results demonstrated that **3** forms hydrogen bond between the pyrazole NH group and carbonyl oxygen as well as coordination bond between the pyrazole nitrogen and central zinc(II) ion, which affords the large stability in the host−guest complex (Scheme 2). From a comparison of the enthalpy changes upon formation of **3**-pyrazole[31] and **4**-pyrazole complexes, the contribution of hydrogen bonding in the binding events of **3** with pyrazole was estimated to be 2.42 kcal/mol, which is large enough for one hydrogen bond, suggesting the suitable geometry of the host porphyrin for the axially coordinated pyrazole.

The titration of **3** with pyrazole was also studied by ^{1}H NMR spectroscopy. In the mixture of **3** and pyrazole, pyrazole protons were observed in the higher magnetic field region than pyrazole alone, indicating the axial coordination of the pyrazole ligand. The pyrazole protons were observed as single species with varying chemical shifts during the course of titration, suggesting that free **3** and **3**-pyrazole complexes are in rapid equilibrium as in other ordinary zinc(II) porphyrin−axial ligand systems. In addition, the following noticeable features were observed for the signals of **3** in the course of the titration with pyrazole as shown in Figure 1. First, ethyl proton signals of the ethoxycarbonyl substituent, observed at −0.29 (CH_3−) and 3.22 ppm (−CH_2−) in the absence of pyrazole, showed a downfield shift upon adding pyrazole and appeared at 0.94 and 3.72 ppm,

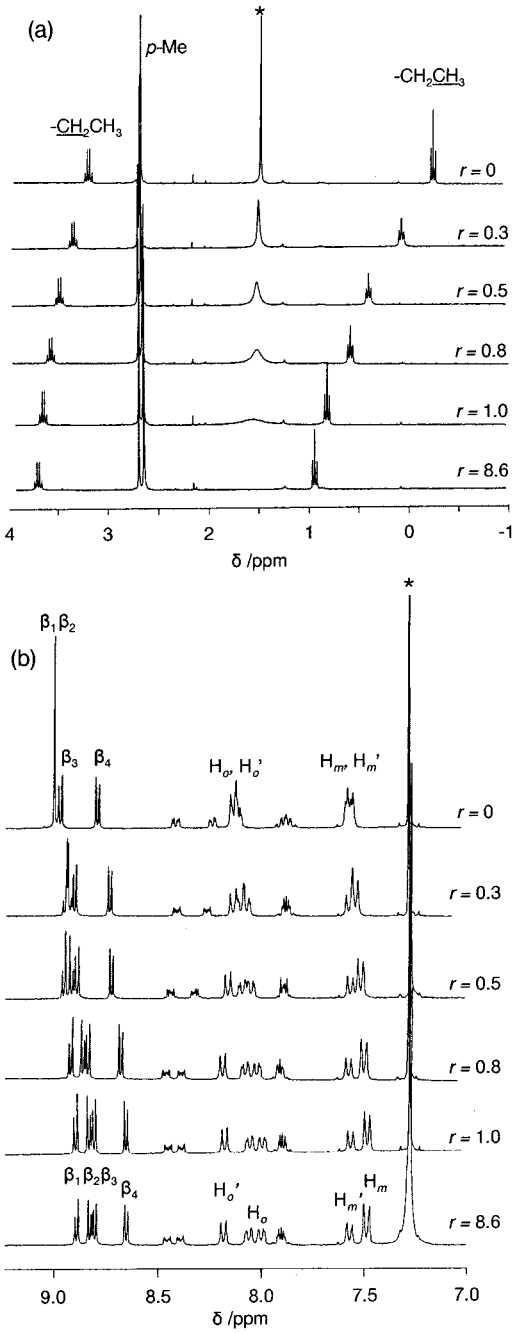

Figure 1. (a) High field, (b) low field regions of the ^{1}H NMR spectra in the course of titration of **3** (5.0×10^{-3} M in $CDCl_3$ at 22 °C) with pyrazole. The mole ratios are shown as r = [pyrazole]/[**3**]. Asterisks denote the residual solvent peak and impurity of H_2O.

respectively, when 9 equiv of pyrazole was added (Figure 1a). These shifts were ascribed to the conformational change of the ethoxycarbonyl group in the minimum energy structure. The original conformation in which the ethyl group is over the porphyrin core, judging from the unusual upfield-shift of the ethyl signals, is changed to the second conformation in which the ethyl group is forced to face outside by the rotation of the $C_{ortho} - C_{carbonyl}$ bond to form the hydrogen bond with pyrazole efficiently (Scheme 2). The structure of the **3** and **3**-pyrazole complex was optimized by the PM3-MNDO method to support the above interpretation (Figure s1 and s2, see Supporting Information). Second, the aryl protons such as H_o, H_m, and *p*-Me in the *p*-tolyl goup at the 10- and 20-*meso* positions showed a gradual upfield shift and became nonequivalent to those in the 15-meso positions. In addition, H_o of the 10,20-tolyl group

(30) The IR spectra were recorded in CCl_4 solution (20 mM) in the presence or absence of 1000 equiv of pyrazole.
(31) **3**-Pyrazole denotes **3** with the pyrazole ligand axially coordinated.

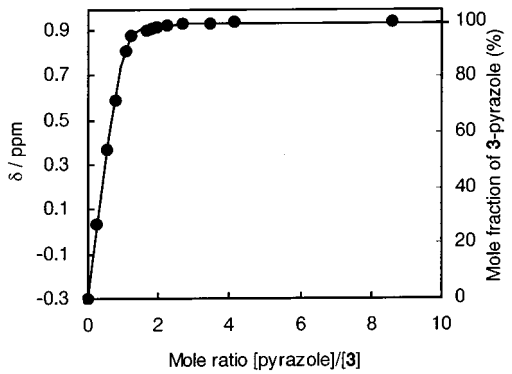

Figure 2. Variation of methyl proton chemical shifts in the titration of **3** with pyrazole (5.0×10^{-3} M in $CDCl_3$ at 22 °C). Calculated curves ($K = 1.8 \times 10^4$ M^{-1}) are shown as solid lines.

exhibited further splitting to two doublets corresponding to the two protons of each other. These splittings were accompanied by the changes in the pyrrole-β_1 and β_2 protons, although these are equivalent and observed as a singlet peak in the absence of pyrazole, but became nonequivalent to each other and appeared separately at 8.87 and 8.80 ppm at the end of the titration as shown in Figure 1b.

These two remarkable features, conformational change in the ethyl chain and splitting of pyrrole-β and aryl protons, were not observed upon adding pyridine to **3,** indicating that the rotation of the axially coordinated pyrazole ligand along the coordination bond is restricted in the ^{1}H NMR time scale due to the formation of the hydrogen bond. The fixed geometry of the pyrazole will cause the upfield shift of aryl protons at the 10- and 20-*meso* positions and nonequivalence between the pyrrole-β_1 and β_2 protons by the ring current effect of the aromatic pyrazole ring. The *meso*-phenyl group does not undergo free rotation at ambient temperature[32] and thus the split of ortho protons in the *p*-tolyl group at the 10- and 20-meso positions is ascribed to the protons situated at the same and opposite side with respect to the porphyrin plane. Furthermore, the binding constants between **3** and pyrazole evaluated from the changes in the ethyl proton chemical shift appeared to be 1.8×10^4 M^{-1} at 22 °C (Figure 2) and agreed with the results from the UV−vis titration ($K = 1.14 \times 10^4$ M^{-1}). These results observed in the ^{1}H NMR titration also showed that the chemical shift of ethyl protons can be used as a diagnostic of the hydrogen bond between the pyrazole and ethoxycarbonyl group in this system.

Determination of the Self-Assembled Structure. To determine the molecular weight of self-assembled products in which relatively weak bond holds each molecule together, VPO or ESI-MS is known as a powerful means.[33] The VPO measurements of **1** and **2** in deuteriochloroform solutions between 5 and 20 mM gave a molecular weight of 2210 ± 100 and 1927 ± 180, corresponding to a trimer of **1** ([**1**]$_3$, FW = 2304.63 g mol^{-1}) and **2** ([**2**]$_3$, FW = 2130.50 g mol^{-1}), respectively. The ^{1}H NMR and UV−vis spectroscopic studies revealed that the self-assembly process of **1** and **2** is almost completed in the concentration rage of VPO measurements (above 99% and 95%, respectively, vide infra) and thus the self-assembled trimeric structures are evident for both compounds. The ESI-MS spectra also gave the peaks at *m*/*z* 2304.5 for **1** and *m*/*z* 2130.7 for **2** to support the formation of trimer [**1**]$_3$ and [**2**]$_3$, although the highest peaks in intensity were monomeric peaks.[34] In fact, trimeric structures for these pyrazolylporphyrins were predictable because our previous study demonstrated that an analogous pyrazolylporphyrin to **2** forms a trimer.[8f] These results indicated that **1** having an additional functional group forms a similar assembled structure to that of the trimer of **2**.

Figure 3 shows the ^{1}H NMR spectra of [**1**]$_3$ recorded in CD_2Cl_2. All the peaks were assigned using H−H COSY measurements and the pyrazole NH peak was assigned by deuteration of the peak by mixing a few drops of deuterioxide into the sample solvent. In contrast to the ^{1}H NMR spectra of corresponding free-base porphyrin **11**, **1** showed a spectral pattern characteristic of self-assemblies. First, large upfield shifts were observed for pyrazole ring protons and pyrrole-β protons as observed previously for axially coordinated self-assemblies.[12−14] The magnitude of upfield shifts, $\Delta\delta$,[35] for pyrazole-H_3 and -H_5 is 5.80 and 1.88 ppm, and that for pyrrole-β_1 and $-\beta_2$ is 1.74 and 0.26 ppm, respectively. These upfield shifts are explained by the ring current effect of the porphyrin macrocycle which is caused by the close proximity of these protons above the porphyrin core. Therefore, the formation of coordination bond between pyrazole nitrogens and zinc(II) ions in the porphyrin core was confirmed in the self-assembly. The *ortho* protons in the *p*-tolyl groups at the 10- and 20- position observed at 8.08 ppm for **11** now split into two signals at 7.97 and at 8.34 ppm in [**1**]$_3$. These splittings were also observed in the model system of **3**-pyrzole, but the enhanced splittings indicate the strong ring current effect from the neighboring porphyrin macrocycles. Therefore, the two split signals of *ortho* protons were ascribed to the protons oriented to the outer sphere of the trimer core and to the other protons directed to the center of the core, respectively. This agrees with the closed cyclic trimer structure in which the inner and outer parts of *p*-tolyl protons are situated in a different environment.

The ^{1}H NMR spectra of [**1**]$_3$ were essentially concentration independent in the concentration range of NMR measurements (10^{-2} to 10^{-4} M) to evidence the large stability of its trimer. This is in contrast to the case for [**2**]$_3$ in which the ^{1}H NMR spectra show large concentration dependencies and the self-assembling process is almost completed only above 100 mM. The difference observed for self-assembling tendencies between **1** and **2** is most likely caused by the contribution of hydrogen bonding. Indeed, formation of the hydrogen bond was confirmed by the IR spectra of carbonyl and pyrazole NH of [**1**]$_3$ observed at 1707.1 and 3330.6 cm^{-1}, respectively, in dichloromethane (10^{-3} M). These stretching bands are lower in frequencies compared with those of the monomer of free base porphyrin **11** ($\nu_{C=O}$ = 1718.3 cm^{-1} and ν_{NH} = 3452.0 cm^{-1}), indicating the hydrogen bonding between pyazole NH and carbonyl oxygen of the ethoxycarbonyl substituent. In addition, formation of hydrogen bond in [**1**]$_3$ was also estimated from the ^{1}H NMR chemical shift compared with those of the model compound **3** because the "diagnostic" downfield shifts were observed for the ethyl protons on going from free base **11** to the zinc(II) complex **1**: the $\Delta\delta$ values for methyl and methylene protons of the ethyl group were 1.46 and 0.57 ppm, respectively. Considering the concentration independencies and the diagnostic shifts of the

(32) La Mar, G. N.; Eaton, G. R.; Holm, R. H.; Walker, F. A. *J. Am. Chem. Soc.* **1973**, *95*, 63.

(33) (a) Shetty, A. S.; Zhang, J.; Moore, J. S. *J. Am. Chem. Soc.* **1996**, *118*, 1019. (b) Drain, C. M.; Fischer, R.; Nolen, E. G.; Lehn, J.-M. *J. Chem. Soc. Chem. Commun.* **1993**, 243. (c) Fujita, M.; Nagao, S.; Ogura, K. *J. Am. Chem. Soc.* **1995**, *117*, 1649. (d) Olenyuk, B.; Whiteford, J. A.; Fechtenkötter, A.; Stang, P. J. *Nature*, **1999**, *398*, 796.

(34) The molecular peak of [**2**]$_3$ was more difficult to detect due to its smaller binding constant than that of [**1**]$_3$. The molecular peak of [**1**]$_3$ was observed using CH_2Cl_2 as eluent at 22 °C, while that of [**2**]$_3$ was only observed using EtOAc/AcOH as eluent at 22 °C.

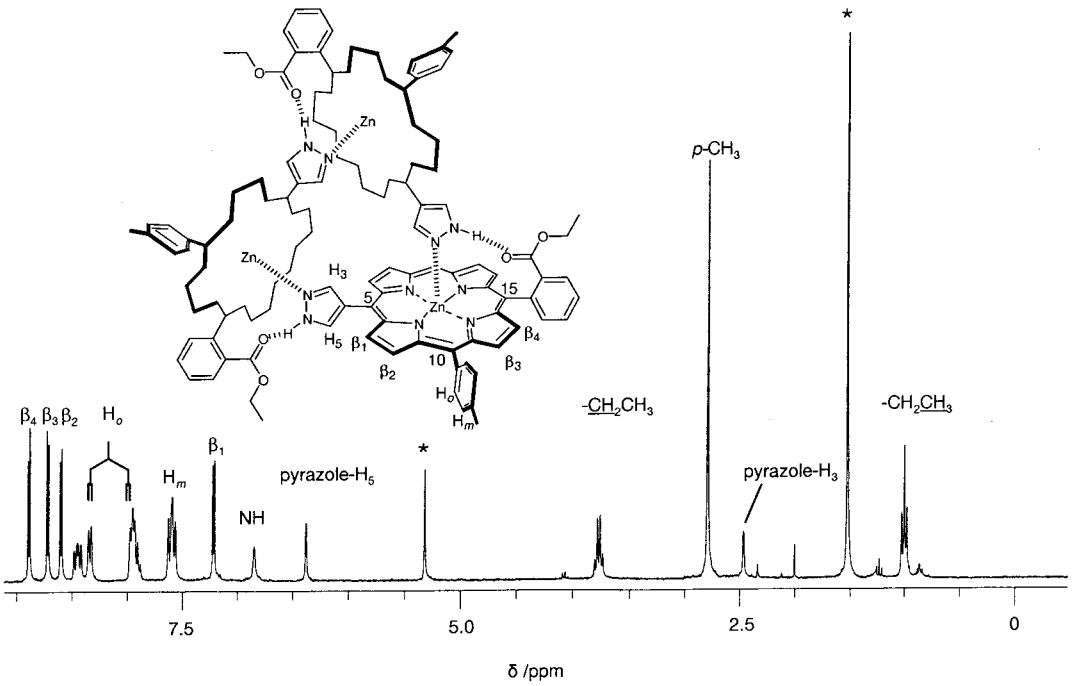

Figure 3. ^{1}H NMR spectrum of the trimer $[\mathbf{1}]_3$. Asterisks denote the residual solvent peak and impurity of H_2O. The total concentration of **1** is 4 $\times$ 10^{-3} M. *p*-Tolyl groups at the *meso*-20 position are omitted for clarity in the insert.

ethyl proton signals of **1**, the formation of a hydrogen bond between pyrazole NH and carbonyl oxygen as well as coordination between pyrazole nitrogen and the zinc(II) ion should be complete in the experimental concentration range of the NMR measurements. Consequently, it was confirmed that the cyclic trimer $[\mathbf{1}]_3$ structure is held together by three coordination bonds and three hydrogen bonds. A space-filling model revealed that the trimer has a compact structure with a small core but without severe steric repulsion (Figure S6).

Determination of the Binding Constant for the Trimer. Figure 4 shows the UV−vis spectra of **1** and **2** recorded in various concentrations. As the concentration was decreasing, the Soret band became sharper and both Soret and Q-bands were blue shifted with isosbestic points at 411, 427, 556, and 580 nm. These spectral changes may be induced by the coordination of the pyrazole nitrogen to the adjacent zinc(II) ion and/or by the porphyrin−porphyrin interaction through the proximity of the porphyrin plane in the closely packed trimer structure.

As indicated in the ^{1}H NMR spectra, a comparison of the absorption spectral changes in **1** and **2** suggests that the affinity constant of **1** is apparently larger than that of **2.** The gradual spectral change in **2** is caused by dissociation below 10^{-3} M and results in a virtually monomeric spectrum at 10^{-5} M, while the spectral change in **1** provides no proof of dissociation above 10^{-5} M to suggest the formation of a stable trimer. These spectral changes are consistent with the facts that the ^{1}H NMR spectra of **1** are independent of the concentration while those of **2** depend on the concentration. The equilibrium constants for the formation of a trimer, K_3, were determined by the curve fitting analysis[10a,36] for the changes in molar absorption coefficients observed at the Soret band (421 nm for **1**) and Q-band (522 nm for **2**) upon dilution.[37] The dilution curves of **1** and **2**

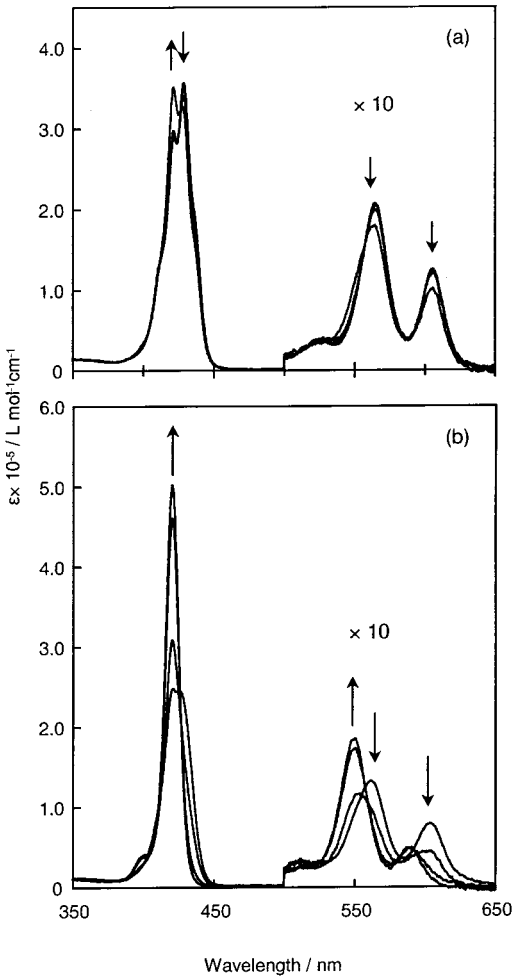

Figure 4. Absorption spectra of (a) **1** and (b) **2** recorded in dichloromethane at 22 °C in 1 $\times$ 10^{-3}, 1 $\times$ 10^{-4}, 1 $\times$ 10^{-5}, and 1 $\times$ 10^{-6} M using 0.025, 0.1, 1.0, and 10 mm path length cells. Arrows indicate the spectral change upon dilution.

(35) $\Delta\delta$ is defined as $\delta(\mathbf{11}) - \delta(\mathbf{1})$.
(36) Saunders, M.; Hyne, J. B. *J. Chem. Phys.* **1958**, *29*, 1319.
(37) The changes in observed molecular absorption coefficients at B-band (421 nm, for **1**) and Q-band (552 nm, for **2**) were used. The binding constants for **2** could be obtained from the concentration-dependent ^{1}H NMR spectra.

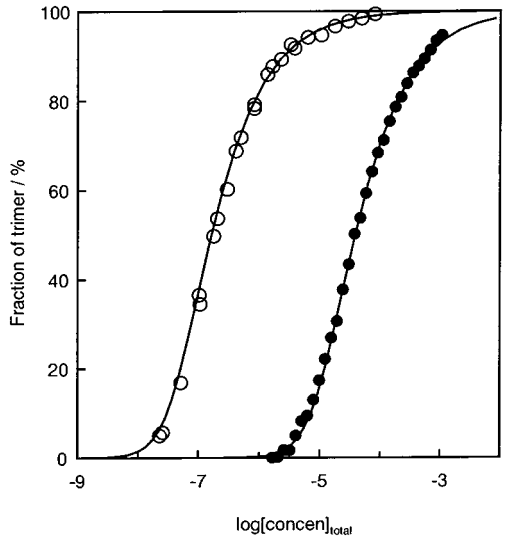

Figure 5. Aggregation curves for **1** (○) and **2** (●) in dichloromethane at 22 °C derived from the absorption spectral changes upon dilution (see text). Solid lines are calculated by assuming trimer formation.

Table 2. Thermodynamic Parameters of Trimer Formation in Dichlromethane[a]

	T (°C)	K_3 (M^{-2})	ΔG (kcal mol^{-1})	ΔH (kcal mol^{-1})	$T\Delta S$ (kcal mol^{-1})
$[\mathbf{1}]_3$	2	$(2.3 \pm 0.5) \times 10^{15}$			
	12	$(3.3 \pm 0.5) \times 10^{14}$			
	22	$(6.0 \pm 0.8) \times 10^{13}$	−18.7	−27.8	−9.12
	33	$(1.3 \pm 24) \times 10^{12}$			
$[\mathbf{2}]_3$	2	$(3.5 \pm 0.5) \times 10^{9}$			
	12	$(9.0 \pm 0.7) \times 10^{8}$			
	22	$(2.8 \pm 0.1) \times 10^{8}$	−11.4	−20.3	−8.91
	33	$(8.0 \pm 0.7) \times 10^{7}$			

[a] Free energy (ΔG) and entropy changes ($T\Delta S$) are calculated at 22 °C.

were in good agreement with the calculated model based on the formation of a trimer and the simulated curves for both compounds are shown in Figure 5. From these analyses, K_3 for **1** at 22 °C was estimated to be $(6.0 \pm 0.8) \times 10^{13}$ M^{-2} which is much larger than $(2.8 \pm 0.1) \times 10^{8}$ M^{-2} for **2**, indicating the significant contribution of the hydrogen bonding to the trimerization constant K_3. The K_3 of **1** is larger than that of the well-designed cyclic zinc(II) trimer ($K_3 = 5 \times 10^{12}$ M^{-2}) where coordination between the pyridine substituent and zinc(II) ion in the porphyrin core holds each other.[8e] This also proves the large contribution of the hydrogen bond because the coordination of pyrazole ($pK_a = 2.5$)[38] is much weaker than that of pyridine ($pK_a = 5.29$). The curve fitting analyses were also carried out in the range of 275−306 K, which gave the linear relationship between $1/T$ and ln K in the van't Hoff plots. The thermodynamic parameters, ΔG, ΔH, and $T\Delta$S in dichloromethane are summarized in Table 2. As expected, **1** showed negatively larger ΔG and ΔH values than **2**, suggesting the favorable contribution of the hydrogen bond in the trimer. The entropy changes in **1** is negatively larger compared with those in **2,** which may be ascribed to the disturbance of the free rotation of the ethoxycarbonyl substituent due to the hydrogen bond and thus to the certain loss of entropy. If we assume that the enthalpy changes in the formation of $[\mathbf{1}]_3$ by the coordination bond are in the same magnitude as in $[\mathbf{2}]_3$, the contribution of the hydrogen bond can be evaluated as 7.50 kcal per molar trimer from the difference in the enthalpy changes of $[\mathbf{1}]_3$ and $[\mathbf{2}]_3$.[39] Therefore, the energy of one hydrogen bond in $[\mathbf{1}]_3$ could be estimated to be 2.50 kcal mol^{-1}. This bond energy is nearly the same in magnitude as the energy of the hydrogen bond observed in the **3**-pyrazole model system (2.42 kcal mol^{-1}), indicating that the hydrogen bond is effectively formed in the trimer as well. On the other hand, the energy of one coordination bond in the trimer, 6.77 kcal mol^{-1}, estimated by dividing the ΔH in $[\mathbf{2}]_3$ by three, is smaller than that observed in the model system of **4**-pyrazole (9.15 kcal). This difference may be induced by the different basicity between pyrazole itself and 4-pyrazolyl group and/or by some geometrical strain in the trimer structure such as tilting of the pyrazole plane against the coordination bond and the rotation of the pyrazole substituent along the *meso* bond.

Spectroscopic Properties of the Trimer. It is well-known that the close spaced porphyrin assembly shows a characteristic absorption spectra due to the intermolecular interaction explained by exciton coupling theory.[40] For example, the blue shift in cofacial dimer arrangement and the band splitting in head-to-tail arrangement were studied thoroughly.[10a,41] The splitting of Soret band in a cyclic trimer[8e] and the broadening in a cyclic tetramer[9] were also reported. In the present study, $[\mathbf{1}]_3$ exhibited enough stability for the optical measurements in dilute solution. The trimerization constant K_3 revealed that more than 95% of **1** exists as a trimer in 10^{-5} M and over 85% in 10^{-6} M in dichloromethane solution at 22 °C. The trimer $[\mathbf{1}]_3$ showed a split Soret band at 421 and 429 nm above 10^{-6} M, but shoulder peaks appeared at both sides of the Soret band, indicating the presence of the other peaks. The peak deconvolution analysis for the Soret band region of $[\mathbf{1}]_3$ in 6×10^{-6} M clearly showed that there are five Gaussian peaks (Figure 6a).[42] Among these peaks, four peaks at 414, 421, 428, and 436 nm with the peak area ratio 0.9:0.9:1.1:1.0, respectively, are ascribed to the Soret band (B(0,0) band) and a broad peak around 410 nm is to B(1,0) band[43] because the former four peaks gradually become one sharp, intense single peak at 430 nm that is characteristic of the Soret band while the peak at 410 nm does not change upon dissociation of the trimer into the corresponding monomer by adding excess pyrazole(Figure S7). All of the above considerations indicated that the four peaks are ascribed to the Soret band of $[\mathbf{1}]_3$ and the four components are due to the exciton coupling in the trimer. These results are interesting because most of the reported porphyrin oligomers with split Soret bands have only two peaks and the Soret band in the reported dimer systems can be fit to two Gaussian peaks.[41a,b] Another explanation of the split Soret band is that the four peaks are resulting from the mixing of several different species such as residual monomers and dimers which have different absorption maxima. Indeed, the Soret band of **1** under dilute conditions ($\lambda_{max} = 420$ nm,

(38) Potts, K. T. *Comprehensive Heterocyclic Chemistry*; Pergmon Press: Oxford, 1984.

(39) In fact, the contribution of the hydrogen bond may vary to some extent because the cooperative effect in the simultaneous formation of hydrogen bond and coordination is included and the coordination (Lewis acidity of the metal) of **1** is expected to be slightly weaker than that of **2** in view of the results from the model system (see Table 1).

(40) Kasha, M.; Rawls, H. R.; El-Bayoumi, M. A. *Pure. Appl. Chem.* **1965**, *11*, 371.

(41) (a) Osuka, A.; Maruyama, K. *J. Am. Chem. Soc*. **1988**, *110*, 4454. (b) Nagata, T.; Osuka, A.; Maruyama, K. *J. Am. Chem. Soc*. **1990**, *112*, 3054. (c) Hunter, C. A.; Sanders, J. K. M.; Stone, A. J. *Chem. Phys*. **1989**, *133*, 395.

(42) The deconvolution analyses were carried out on the spectra in the wavenumber scale, but the results are shown in the wavelength scale for convenience.

(43) Gouterman, M. *The Porphyrins*; Dolphin, D., Ed.; Academic Press: New York, 1978; Vol. III, pp 1−165.

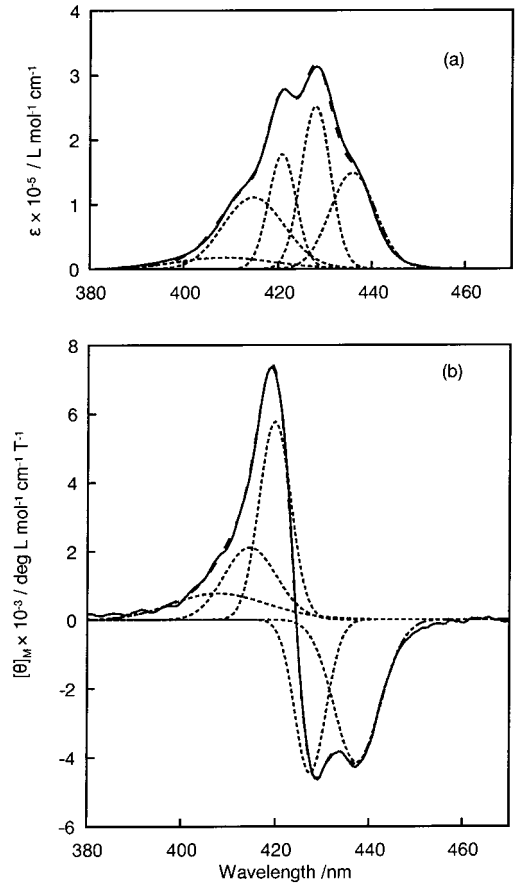

Figure 6. Deconvolution analysis of (a) absorption spectra and (b) MCD spectra of **1** (6.3 × 10^{-6} M in dichloromethane, 22 °C): (—) experimental data; (- - -) fitted data; (- - -) individual bands.

10^{-8} M) appeared near to the one of the deconvoluted peaks. However, this assumption is unlikely because the peak position and ratio of the four bands did not show any concentration dependencies above 10^{-5} M to 10^{-3} M although they should be observed if there exist several species in equilibrium. The ^{1}H NMR spectral pattern ascribed to a single species also denied that possibility. Another possibility that the trimer has several conformations with different λ_{max} is also ruled out because such a conformational change should give rise to additional resonance in ^{1}H NMR. This is not the case and apparently different from our observation.

To obtain more detailed information about the optical properties, the MCD spectra were recorded. In general, a Faraday A term appears in metalloporphyrins with D_{4h} symmetry when the excited states are degenerate. Indeed, the dissociated monomer **1**-pyrazole complex in D_{4h} symmetry showed a characteristic Faraday A term for both Soret and Q-band (data not shown). On the other hand, the trimer [**1**]$_3$ showed a distinct Faraday B term in the Soret band region (Figure 6b). Peak deconvolution analysis showed five Gaussian peaks corresponding to those in the UV−vis spectra with nearly the same λ_{max} and bandwidth.[44] The appearance of the Faraday B term induced by the mixing of the ground and excited states with other electronic states under the influence of the external magnetic field[45] indicates two sets of the interaction between the transitions appearing at 414 and 421 nm and the interaction between the transition observed at 428 and 436 nm.[46] This is clear evidence for the exciton coupling in the Soret band and a reason [**1**]$_3$ exhibits four split Soret bands. It is well-known that the Soret band has two perpendicular components B_X and B_Y.[43] Since the Faraday B term shows corresponding X and Y transition in opposite signs, the observed MCD spectra showed that each of the B_X and B_Y transitions have two components. These results indicated that three transition dipole moments in the X or Y direction interact with each other in the trimer to cause the two allowed exited states in both direction. If we place the B_X transition along the 10,20-axis and B_Y transition along the 5,15-axis, three B_X transitions are parallel orientation and three B_Y are oblique in triangle orientation. According to the theory developed by Kasha,[40] the cyclic trimer transition dipole array has only partially split character in the exciton diagram and the lower exciton state always has some forbidden character. In our experiments, forbidden characters seemed to be weakened since the observed four peaks have nearly the same peak integrated ratios. This is probably due to the lower symmetry of our trimer (C_3) compared with that of model system (D_{3h}) used by Kasha.

On the other hand, no distinct differences were observed in the UV−vis and MCD spectra of [**1**]$_3$ and **1**-pyrazole in the Q-band region. The Q-band of [**1**]$_3$ observed at 564 and 605 nm are quite similar to those of **1**-pyraozole (565 and 607 nm). In addition, the Faraday A term observed for the Q-band of [**1**]$_3$ and **1**-pyrazole suggested that the exciton coupling in the Q-band region is weak compared to that in the Soret band. The less pronounced exciton coupling in the Q-band is ascribed to the weak absorption intensity of the Q-band compared to the Soret band because the exciton splitting energy is directly related to the square of the magnitude of the transition moment.[40]

The fluorescence emission spectra of [**1**]$_3$ ($\lambda_{fluor\ max}$ = 613 nm, Φ_f = 0.021)[47] showed much the same spectral properties as observed for **1**-pyrazole ($\lambda_{fluor\ max}$ = 616 nm, Φ_f = 0.020). Interestingly, [**1**]$_3$ gave the same Φ_f value as **1**-pyrazole, suggesting that the emission from [**1**]$_3$ is not quenched despite close proximity in the trimer structure. This is in contrast to strong quenching in the cofacial dimer arrangement.[41a,48] The flouorescence decay profiles of [**1**]$_3$ and **1**-pyrazole were essentially single exponential to give lifetimes almost identical with that of the monomeric zinc(II) porphyrin (1.42 ns for [**1**]$_3$ and 1.34 ns for **1**-pyrazole). These results indicate the absence of the significant perturbation in their S_1 state despite the strong interaction in their S_2 states.

Electrochemical Properties. To clarify the electronic communication in the trimer, the cyclic voltammogram and differential pulse voltammogram were measured for **1** under 10^{-3}

(44) The differences in λ_{max} or half-bandwidth between corresponding Gaussian peaks in UV−vis and MCD spectra were within 1.5 nm. In a precise sense, bandwidths and band maxima will be the same in both absorption and MCD spectra, but the small differences could not be avoided in our experiments since the fitting procedures were done individually. For the elaborated deconvolution analysis, see: (a) Nyokong, T.; Gasyna, Z.; Stillman, M. J. *Inorg. Chem.* **1987**, *26*, 1087. (b) Browett, W. R.; Stillman, M. J. *Comput. Chem.* **1987**, *11*, 241.

(45) Sutherland, J. C. *The Porphyrins*; Dolphin, D., Ed.; Academic Press: New York, 1978; Vol. III, pp 225−248.

(46) For the MCD studies of porphyrin assemblies that exhibit exiton coupling, see: (a) Sugiura, K.; Ponomarev, G.; Okubo, S.; Tajiri, A.; Sakata, Y. *Bull. Chem. Soc. Jpn.* **1997**, *70*, 1115. (b) Ohta, K.; Azumane, S.; Kawahara, W.; Kobayashi, N.; Yamamoto, I. *J. Mater. Chem.* **1999**, *9*, 2313.

(47) The emission spectra were recorded at a total concentration of ca. 10^{-6} M (Abs$_{\lambda exc}$ < 0.1). Quantum yields were calibrated using ZnTPP (Φ_f = 0.03) as a standard. (Seybold, P. G.; Gouterman, M. *J. Mol. Spectrosc.* **1969**, *31*, 1.) Both compounds also showed nearly the same emission properties at an increased concentration of 10^{-5} M.

(48) Hunter, C. A.; Leighton, P. L.; Sanders, J. K. M. *J. Chem. Soc., Perkin Trans. 1* **1989**, 547.

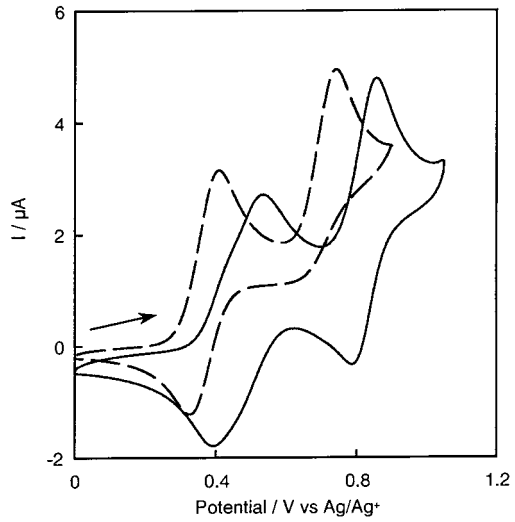

Figure 7. Cyclic voltammograms of $[\mathbf{1}]_3$ (solid line) and **1**-pyrazole (broken line) in 0.1 M TBA(BF_4) dichloromethane solution. The total concentration of **1** is 1×10^{-3} M in both cases.

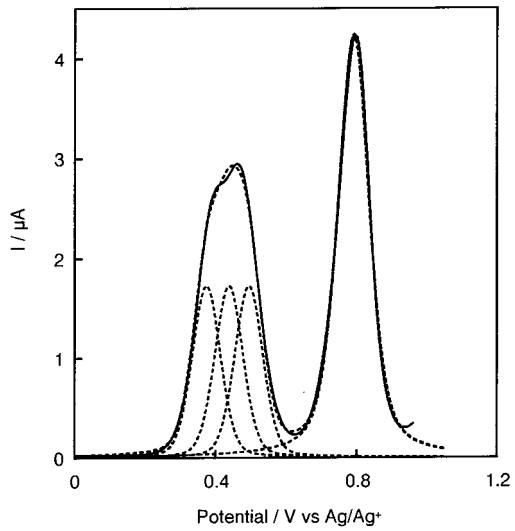

Figure 8. Differential pulse voltammogram of $[\mathbf{1}]_3$ in 0.1 M TBA(BF_4) dichloromethane solution. Deconvoluted peaks and fitted data are shown in broken line.

M where **1** exists as a trimer $[\mathbf{1}]_3$ (Figures 7 and 8).[49] The measurements were also carried out for the corresponding monomer, i.e., **1**-pyrazole using the same solution of **1** but containing 1000 equiv of pyrazole. Both porphyrins showed two oxidation states ascribed to the first and second oxidation process of the porphyrin ring with several characteristics of the assembly. First, from a comparison of the voltammogram between $[\mathbf{1}]_3$ and **1**-pyrazole, the first and second ring oxidations of the trimer occurred in more anodic potentials than that of the monomer. This difference may be due to the delocalization of the remaining electron of the π-cation radical over the cyclic trimer structure. Alternative explanation for the different potentials is based on the difference in the pK_a between the pyrazole ligand in **1**-pyrazole and the pyrazolyl substituent in $[\mathbf{1}]_3$ because the axial ligand with a large pK_a value makes the oxidation potential less anodic.[50] In contrast to **1**-pyrazole with a reversible first porphyrin ring oxidation wave ($E_{1/2} = 0.38$ V), a broad redox wave ($E_p = 0.39$ and 0.53 V) of the first oxidation process was observed for $[\mathbf{1}]_3$. DPV measurements also showed a broad peak with asymmetric shape for this process, suggesting the splitting of the oxidation potential in the trimer. Peak deconvolution analysis showed that the experimental results are in good agreement with the assumption that the peak is composed of three components ($E_p = 0.35$, 0.44, and 0.49 V) with the same peak intensity and width (Figure 8).[51] These results indicated that the first porphyrin ring oxidation split into three potentials due to the electronic interaction within the trimer. This splitting is known to be affected both by the distance between the porphyrin rings and by the molecular orbital distribution in the porphyrin core.[9,13f,52] The difference between the split oxidation potentials in the first porphyrin ring oxidation process is 86 and 58 mV from the peak deconvolution analysis. These are the intermediates between mutually coordinated cofacial dimer ($\Delta E = 200-450$ mV)[52b,c] and cyclic tetramer ($\Delta E = 28-60$ mV).[9]

As to the second porphyrin ring potential, **1**-pyrazole showed no reduction process coupled to the second oxidation peak at 0.74 V. This behavior is similar to that observed in the ZnTPP−pyridine system[53] and is ascribed to the formation of isoporphyrin by nuceophilic substitution of the excess pyrazole to the dication species.[54] On the other hand, formation of isoporphyrin did not occur in $[\mathbf{1}]_3$ since the pyrazolyl substituent was coordinated to the adjacent porphyrin core. This process resulted in a one-step three-electron wave ($\Delta E_p = 65$ mV) in contrast to the stepwise oxidation in the first oxidation potential, indicating that there exists virtually no interaction in this step.

Conclusions

A novel cyclic trimer of zinc(II) pyrazolylporphyrin has been constructed by the molecular recognition approach using coordination and hydrogen bonding. Spectroscopic studies have revealed that three hydrogen bonds (2.50 kcal per one bond) and three coordination bonds (6.77 kcal per one bond) support the trimer and effectively afford the stable trimer with the overall formation constants of 6.0×10^{13} M^{-2} at 22 °C. This trimer exhibits a characteristic absorption spectral pattern: Each exited state of B_X and B_Y splits into two allowed transition states by exciton coupling to yield four components in the Soret band. The fluorescent quenching of the trimer has not been observed despite the close proximity of the porphyrin rings in the trimer structure. Electrochemical studies suggest the splitting of the first oxidation potential of the porphyrin ring. It may be possible to extend this approach to higher, elaborated oligomers such as larger ring shaped assemblies by modifying the pyrazolyl

(49) Dissociation of the trimer by supporting electrolyte was ruled out by the UV−vis spectral pattern of the solution.

(50) Kadish, K. M.; Shiue, L. R.; Rhodes, R. K.; Bottomley, L. A. *Inorg. Chem.* **1981**, *20*, 1274.

(51) The mixed Gaussian−Lorentzian function was used for the deconvolution analyses. The choice of the above function was arbitrary but it seems reasonable because this function showed good agreement with the current−potential curves in the ferrocene−ferrocenium couple or with the split one in the mixed-valence state theoretically drawn by the equation developed by Henry Taube: Richardson, D. E.; Taube, H. *Inorg. Chem.* **1981**, *20*, 1278.

(52) (a) Becker, J. Y.; Dolphin, D.; Paine, L. B.; Wijesekera, T *J. Electroanal. Chem.* **1984,** *164*, 335. (b) Maiya, G. B.; Krishnan, V. *Inorg. Chem.* **1985**, *24*, 3253. (c) Vasudevan, J.; Stibrany, R. T.; Bumby, J.; Knapp, S.; Potenza, J. A.; Emge, T. J.; Schugar, H. J. *J. Am. Chem. Soc.* **1996**, *118*, 11676. (d) Ogawa, T.; Nishimoto, Y.; Yoshida, N.; Ono, N.; Osuka, A. *Angew. Chem., Int. Ed.* **1999**, *38*, 176.

(53) Kadish, K. M.; Rhodes, R. K. *Inog. Chem.* **1981**, *20*, 2961.

(54) The possibility of the nucleophillic substitution for the pyrrole-β position seemed to be ignored in this solvent system. See ref 53 and: (a) Kahef, L. E.; Meray, M. E.; Gross, M.; Giraudeau, A. *J. Chem. Soc., Chem. Commun.* **1986**, 621. (b) Kalhef, L. E.; Gross, M.; Giraudeau, A. *J. Chem. Soc., Chem. Commun.* **1989**, 963.

substituent that may have potentiality to mimic some aspects of natural photosynthesis.

Acknowledgment. We are grateful to Professor Taira Imamura and Dr. Kenji Watabe at Hokkaido University for their kind help with the ESI mass spectrometry and Professor Masao Kaneko at Ibaraki University for kind help for the fluorescence lifetime measurements. C.I. thanks Keio University for financial support.

Supporting Information Available: Synthetic procedure for compounds **2**, **3**, **6**, and **13**, H−H COSY spectrum of [**1**]$_3$, ^{1}H NMR spectrum of **2**, a figure showing the concentration dependencies of **2** in ^{1}H NMR spectra, and the optimized structures of **3**,**3**-pyrazole and [**1**]$_3$. This material is available free of charge via the Internet at http://pubs.acs.org.

IC001421K